

Metaprism-aided NLOS Target Localization

Marina Lotti and Davide Dardari
DEI, University of Bologna and WiLab-CNIT
Cesena Campus (FC), Italy
{marina.lotti2, davide.dardari}@unibo.it

Abstract—In future wireless systems, radar and communication functionalities are expected to be integrated to improve the awareness of the network and enable new applications. To make the radar work even in the presence of obstacles, this paper proposes the use of a passive frequency-selective metasurface, named *metaprism*, to allow a conventional frequency-modulated continuous wave (FMCW) radar to estimate both the range and the angle of a target hidden by an obstacle. Results indicate that it is possible to obtain a very accurate angle and range estimate without involving additional active devices and/or multiple antennas at the radar.

Index Terms—Metaprism, NLOS localization, intelligent surfaces, localization, FMCW radar, ISAC.

I. INTRODUCTION

Recently, the holographic radio concept has been defined as the capability of a wireless system to obtain a holistic perception of the surrounding environment and a way to manipulate, with unprecedented flexibility, the electromagnetic field generated or sensed by an antenna [1]. Towards this concept, next-generation wireless systems are expected to embed typical radar functionality in addition to communication, thus leading to the definition of the integrated sensing and communication (ISAC) concept [2], [3]. A common type of signal used in radar systems is the frequency-modulated continuous wave (FMCW), which is characterized by the transmission of frequency sweeps (chirps) and the estimation of the target's range using low-complexity receivers.

In indoor scenarios with many obstacles (e.g., industrial Internet-of-things (IIoT)), it becomes difficult to locate a target without adding more base stations (BSs) and hence leading to prohibitive costs. An envisaged solution is to deploy in the environment reconfigurable intelligent surfaces (RISs) which are capable of reflecting the signals to create virtual line-of-sight (LOS) conditions [4]–[6]. However, RISs require reconfigurable devices, energy supply, the estimation of the channel state information (CSI), and dedicated control channels. To overcome these drawbacks, in [7], the concept of *metaprism* was introduced to allow communication in non-line-of-sight (NLOS) condition. A metaprism is a passive and non-reconfigurable metasurface that acts as a metamirror and has the property of generating frequency-dependent reflections. In fact, if properly designed, the reflection angle of the signal that impinges the metaprism does not follow the usual Snell law, but it is a function of the signal's characteristics. Therefore, differently from a RIS, it is possible to shape and reflect the signal without having to interact with the metaprism or having to estimate the CSI.

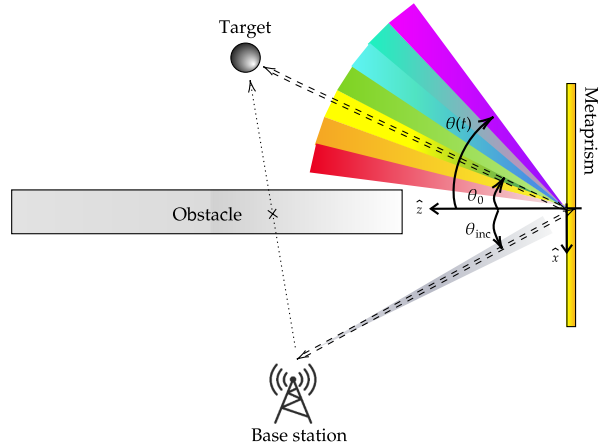


Fig. 1. Reference scenario.

In this work, we show that by using a metaprism it is possible to detect the position of a target hidden by an obstacle using a standard FMCW signal. In particular, we propose an enhanced FMCW receiver capable of jointly estimating with high accuracy the range and angle of the target using a simple-single antenna FMCW radar. The performance of angle estimation is characterized both in terms of the Cramér-Rao bound (CRB) and simulations.

II. SYSTEM MODEL

The reference scenario considered in this paper is shown in Fig. 1, where a BS located at coordinates \mathbf{p}_{BS} operating as a radar generates an FMCW signal to detect and localize a target at position \mathbf{p}_T hidden by an obstacle. To accomplish this task, the BS exploits the reflection through a frequency-selective non-reconfigurable metasurface (the metaprism) which is supposed to be in LOS with respect to both the BS and the target. With reference to the normal of the metaprism, denote by θ_{inc} and θ_0 , respectively, the angle of incidence of the signal generated by the BS and the angle of view of the target along the $x-z$ plane. No particular assumption is made on the BS' antenna that can be a single element or an array. The signal emitted by the FMCW radar is composed of one or more linear frequency modulated (LFM) chirps, i.e., a sinusoidal signal whose frequency varies linearly starting from an initial frequency f_{start} and ending at the final frequency f_{stop} , thus covering the bandwidth $W = f_{stop} - f_{start}$ in a period of

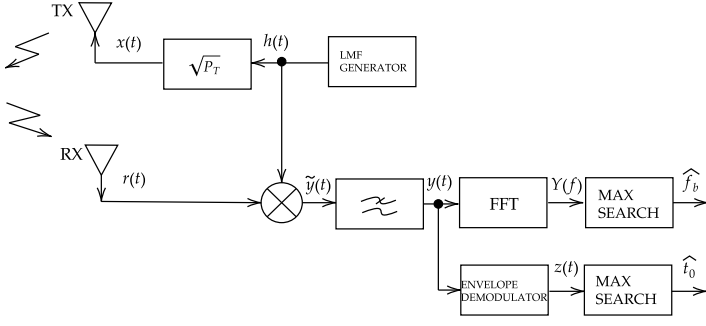


Fig. 2. Modified FMCW transceiver.

duration T (chirp time). The normalized chirp is given by [8]

$$h(t) = \text{rect}\left(\frac{t}{T}\right) \cos(2\pi f(t)t) \quad (1)$$

where $f(t) = f_0 - W/2 + \beta t$ is the instantaneous frequency, with f_0 being the center frequency, β the slope of the FMCW signal, and $\text{rect}(x) = 1$, for $|x| < 0.5$, zero otherwise. The transmitted signal is $x(t) = \sqrt{2P_T} h(t)$, where P_T is the transmitted power.

As it will be described in Sec. III, the metaprism is designed in such a way, for a given incident angle θ_{inc} , the FMCW signal emitted by the BS is reflected towards the angle $\theta(t) = \theta(f(t))$ depending on the instantaneous frequency $f(t)$ of the chirp. As a consequence, the frequency sweep of the chirp translates into an angle sweep of the reflected beam. Assuming the channel does not change within the chirp time, the signal backscattered by the target in the time interval in which the angle of the beam is close to θ_0 is reflected back towards the BS.

We propose now a signal processing scheme capable of estimating both the target angle θ_0 and its distance r_0 from the metaprism, and hence its position, starting from the reflected signal. The signal returned from a stationary target at the range distance r_0 and angle θ_0 is

$$r(t) = \sqrt{2p(t)} \cos(2\pi f(t - \tau)(t - \tau) + \phi_R) + n(t) \quad (2)$$

where ϕ_R is the carrier phase, $n(t)$ is the additive white Gaussian noise (AWGN) with double-side power spectral density $N_0/2$, and $\tau = 2r_0/c$ is the round-trip propagation time with c being the speed of light.¹ $p(t)$ represents the instantaneous received power whose behavior is affected by the metaprism and the target, as it will be clarified in the following. The receiver at the BS is shown in Fig. 2. As in conventional FMCW receivers, the received signal $r(t)$ is mixed with the normalized heterodyne signal generated by the

¹In reality, τ accounts also for the extra delay due to the path between the BS and the metaprism. However, since this is a known quantity, it can always be subtracted then we do not consider it in the following.

LFM generator thus obtaining [8]

$$\begin{aligned} \tilde{y}(t) &= r(t) h(t) \\ &= \sqrt{p(t)} \cos(2\pi(f(t - \tau)(t - \tau) - f(t)t) + \phi_R) + \\ &\quad \sqrt{p(t)} \cos(2\pi(f(t)t + f(t - \tau)(t - \tau)) + \phi_R) + \tilde{w}(t) \end{aligned} \quad (3)$$

where $\tilde{w}(t) = n(t) h(t)$. The signal is then filtered by an ideal low-pass filter with bandwidth W . Note that the choice of W affects the maximum range detectable by the radar as well as the output SNR. After the low-pass filter, all the high-frequency terms are filtered out and the signal becomes

$$\begin{aligned} y(t) &= \sqrt{p(t)} \cos(2\pi(f(t - \tau)(t - \tau) - f(t)t) + \phi_R) + w(t) \\ &= \sqrt{p(t)} \cos(4\pi\beta\tau t + \phi_Y) + w(t). \end{aligned} \quad (4)$$

having defined $\phi_Y = 2\pi f_0\tau - \pi W\tau - 2\pi\beta\tau^2$, and $w(t)$ the filtered version of $\tilde{w}(t)$. The last equation puts in evidence that at the output we obtain a constant frequency signal with frequency [8]

$$f_b = f_b(r_0) = 2\beta\tau = \frac{4r_0\beta}{c} \quad (5)$$

that depends on the target range r_0 . Note that in a conventional FMCW radar setup, i.e., without the metaprism, the instantaneous received power $p(t)$ would be a constant during the reception of one chirp, that is,

$$p(t) = P_R \text{rect}\left(\frac{t - \tau}{T}\right) \quad (6)$$

where P_R is the received power given by the radar range equation. On the contrary, in the presence of the metaprism, the sinusoid in (4) results modulated because, due to the frequency-angular selectivity effect of the metaprism, the signal is reflected by the target only in the time interval close to t_0 , being $t_0 \in [-T/2, T/2]$ the time instant at which the instantaneous frequency $f(t_0)$ corresponds to a reflection of the metaprism towards the target's angle θ_0 , i.e., $\theta(t_0) \approx \theta_0$. We model the instantaneous received amplitude as a delayed version of the waveform $s(t)$ such that $\sqrt{p(t)} = s(t - t_0)$, where the shape of $s(t)$ depends on the target's position, size, and reflection characteristic, and $0 \leq s(t) \leq s(0)$, for $|t| > 0$. Therefore, (4) can be rewritten as

$$y(t) = s(t - t_0) \cos(2\pi f_b t + \phi_Y) + w(t). \quad (7)$$

The output signal (7) can be processed in order to obtain an estimate of the target's range r_0 and angle of view θ_0 . The estimate of the target's range r_0 , through the estimate of f_b , can be obtained according to the classical scheme based on the Fourier transform of $y(t)$ (see the upper branch of the receiver in Fig. 2). In particular, the spectrum of (7) is

$$\begin{aligned} Y(f) &= \frac{1}{2} S(f - f_b) e^{-j2\pi f t_0 + j\phi_Y} + \\ &\quad \frac{1}{2} S(f + f_b) e^{j2\pi f t_0 - j\phi_Y} + W(f) \end{aligned} \quad (8)$$

where $S(f)$ and $W(f)$ are the Fourier transforms of $s(t)$ and $w(t)$, respectively. Specifically, the estimate of f_b can be

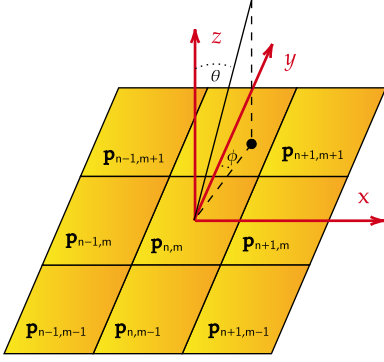


Fig. 3. Geometry of the metaprism.

simply obtained by locating the maximum of $|Y(f)|$. Since the resolution is related to the width of the central lobe of the spectrum around f_b , it is affected by the target position and its characteristics. The main difference with respect to the classical scheme is in the time-dependent power $p(t)$ which decreases the received energy. Regarding the angle θ_0 , it affects the time instant t_0 at which the instantaneous receiver power $p(t)$ presents a peak. Therefore, it is possible to estimate it using the scheme depicted in the lower branch of the receiver in Fig. 2. It consists of an envelope demodulator of the signal $y(t)$ to extract the signal $s(t - t_0)$, that is,

$$z(t) \simeq s(t - t_0) + v(t) \quad (9)$$

followed by a delay estimator consisting of a maximum search, where $v(t)$ is AWGN with power spectral density $G_v(f) = N_0 \text{rect}(f/2W)$ [8], [9]. With the estimated time t_0 , the angle θ_0 of the signal backscattered from the target can be obtained as explained later.

III. METAPRISM DESIGN

A. General model

With reference to Fig. 3, we consider the metasurface in the $x - y$ plane consisting of $N \times M$ cells whose size is $d_x \times d_y$, where $d_x = d_y \approx \lambda/2$, where λ is the wavelength. Denote by $\mathbf{p}_{n,m} = \{x_n, y_m, 0\}$, the position of the nm th cell, where $x_n = n d_x - N d_x/2$, with $n = 0, 1, \dots, N - 1$, and $y_m = m d_y - M d_y/2$, with $m = 0, 1, \dots, M - 1$. The center of the metaprism is $\mathbf{p}_0 = \{0, 0, 0\}$. For an incident plane wave with 3D angle $\Theta_{\text{inc}} = (\theta_{\text{inc}}, \phi_{\text{inc}})$ (azimuth and elevation), the nm -th cell reflection coefficient at the generic 3D observation angle $\Theta = (\theta, \phi)$ can be expressed by the following equation

$$r_{nm}(\Theta_{\text{inc}}, \Theta; f) = \sqrt{F(\Theta_{\text{inc}})F(\Theta)}G_c\Gamma_{nm}(f) = \beta_{nm}(\Theta_{\text{inc}}, \Theta; f)e^{j\Psi_{nm}(f)} \quad (10)$$

where $F(\Theta)$ is the normalized power radiation pattern that accounts for possible non-isotropic behavior of the cell, we model as

$$F(\Theta) = \begin{cases} \cos^q(\Theta) & \theta \in [0, \pi/2], \phi \in [0, 2\pi] \\ 0 & \text{otherwise.} \end{cases}$$

The parameter q depends on the specific technology adopted as well as on the dimension of the cell. $G_c = 4\pi A_{\text{cell}}/\lambda^2$ is the boresight gain of the cell and it was chosen, as in [7], to have

the effective area of the cell equal to the geometric area of the cell. $\Gamma_{nm}(f)$ is the load reflection coefficient, and according to its design it is possible to realize different reflecting behaviors of the metasurface. $\beta_{nm}(\Theta_{\text{inc}}, \Theta; f)$ is the reflection amplitude and $\Psi_{nm}(f)$ is the reflection phase shift of the metasurface. According to the model in [7], $\Psi_{nm}(f)$ can be designed such that it exhibits a linear behavior with the frequency f , i.e.,

$$\Psi_{nm}(f) = \alpha_{nm} \cdot (f - f_0) \quad (11)$$

with $f = f(t)$ being the instantaneous frequency of the FMCW signal, α_{nm} a cell-dependent coefficient. The coefficient α_{nm} can be written in a manner it is related to the position \mathbf{p}_{nm} as

$$\alpha_{nm} = a_0 x_n + b_0 y_m \quad (12)$$

where a_0 and b_0 are two constants that have to be properly designed. As a consequence, the frequency-dependent phase profile results

$$\Psi_{nm}(f) = (a_0 x_n + b_0 y_m) (f - f_0). \quad (13)$$

The relationship between the metaprism's phase profile $\Psi_{nm}(f)$, the angle of incidence Θ_{inc} , and the angle of reflection Θ is

$$\Psi_{nm}(f) = -\frac{2\pi n d_x}{\lambda} (u_x(\Theta_{\text{inc}}) + u_x(\Theta)) - \frac{2\pi m d_y}{\lambda} (u_y(\Theta_{\text{inc}}) + u_y(\Theta)) \quad (14)$$

where we have defined the quantities $u_x(\Theta) = \sin(\theta) \cos(\phi)$ and $u_y(\Theta) = \sin(\theta) \sin(\phi)$. By comparing (13) and (14), we can determine the reflection direction Θ as a function of the frequency f as follows

$$u_x(\Theta) = -u_x(\Theta_{\text{inc}}) - \frac{a_0 \lambda}{2\pi} (f - f_0) \\ u_y(\Theta) = -u_y(\Theta_{\text{inc}}) - \frac{b_0 \lambda}{2\pi} (f - f_0). \quad (15)$$

B. Design example

Suppose that the signal transmitted by the BS impinges the metaprism with incident angle $\Theta_{\text{inc}} = (\theta_{\text{inc}}, 0)$ in the $x - z$ plane, such that $\phi = 0^\circ$. Thus we have $u_x(\Theta) = \sin(\theta)$ and $u_y(\Theta) = 0$. Therefore (15) becomes

$$\sin(\theta) = -\sin(\theta_{\text{inc}}) - \frac{a_0 \lambda}{2\pi} (f - f_0) \quad (16)$$

from which we can obtain the frequency-dependent angle of reflection

$$\theta(f) = \arcsin \left(-\sin(\theta_{\text{inc}}) - \frac{a_0 \lambda}{2\pi} (f - f_0) \right). \quad (17)$$

When illuminated by the chirp signal in (1), the reflected angle becomes time-dependent within the chirp duration T , that is,

$$\theta(t) = \arcsin \left(-\sin(\theta_{\text{inc}}) - \frac{a_0 \lambda}{2\pi} (\beta t - W/2) \right). \quad (18)$$

Now, as an example, we design the coefficient a_0 in (12) in such a way the incident signal from the BS is reflected towards the angle $\theta = -\theta_{\text{inc}} - \theta_m$, when the instantaneous frequency of

the signal is $f_{\text{start}} = f_0 - W/2$ (at the beginning of the chirp), and towards the angle $\theta = -\theta_{\text{inc}}$, when the instantaneous frequency is $f_{\text{stop}} = f_0 + W/2$ (at the end of the chirp). Therefore, θ_m represents the desired angle span necessary to cover the intended NLOS area. From (17) it follows that

$$\begin{aligned} a_0 &= -\frac{2\pi}{\lambda(f_0 - W/2 - f_0)} (-\sin(\theta_{\text{inc}} + \theta_m) + \sin(\theta_{\text{inc}})) \\ &= -\frac{4\pi}{\lambda W} (-\sin(\theta_{\text{inc}} + \theta_m) + \sin(\theta_{\text{inc}})) \end{aligned} \quad (19)$$

and $b_0 = 0$. These values can be used in (12) to obtain the design coefficient of each cell composing the metaprism. Examples of how α_{nm} are related to the specific design of the cell can be found in [7].

C. Link Budget

Assuming the BS and the target in free-space condition with respect to the metaprism, the isotropic two-way channel gain accounting for the metaprism at frequency f is

$$\begin{aligned} G_0(f) &= \frac{\lambda^4 G_c^2 F(\theta_{\text{inc}}) F(\theta_0)}{(4\pi)^4} \left| \sum_{n=0}^{N-1} \sum_{m=0}^{M-1} \frac{\Gamma_{nm}(f)}{\|\mathbf{p}_{\text{BS}} - \mathbf{p}_{nm}\| \|\mathbf{p}_{\text{T}} - \mathbf{p}_{nm}\|} \right. \\ &\quad \left. \exp\left(-j\frac{2\pi f}{c} (\|\mathbf{p}_{\text{BS}} - \mathbf{p}_{nm}\| - \|\mathbf{p}_{\text{T}} - \mathbf{p}_{nm}\|)\right) \right|^2 \end{aligned} \quad (20)$$

where the sum accounts for the $N \cdot M$ elements of the metaprism along the x, y -directions. Γ_{nm} is modeled such that $|\Gamma_{nm}| = 1$ and $\angle \Gamma_{nm} = (f - f_0)(a_0 x_n + b_0 y_m)$. The power intercepted by the target having radar cross-section (RCS) σ_x is:

$$P_{\sigma_x}(f) = P_{\text{T}} G_{\text{T}} G_0(f) G_{\sigma_x}(f) \quad (21)$$

where G_{T} is the antenna gain of the BS, $G_{\sigma_x}(f) = G_{\sigma_x} = \sigma_x 4\pi/\lambda^2$ is the equivalent gain of the target considered as isotropic, as a first approximation. So the power received by the radar becomes

$$P(f) = P_{\sigma_x}(f) G_{\text{T}} G_0(f) = P_{\text{T}} G_{\text{T}}^2 G_0(f)^2 G_{\sigma_x}. \quad (22)$$

Note that during a frequency sweep, $p(t) = P(f(t))$, where $P(f)$ is given by (22).

IV. THEORETICAL PERFORMANCE OF θ_0 ESTIMATION

To obtain an idea of the achievable performance bound in the estimation error variance of the angle θ_0 using the metaprism and the proposed scheme described in Sec.II, we derive the corresponding CRB. Since θ_0 is obtained through the estimation of the intermediate parameter t_0 , we can first compute the CRB on the estimation error variance of t_0 from the classical bound given by [10]

$$\text{CRLB}_{t_0} = \frac{N_0}{2(2\pi)^2 B_{\text{eff}}^2 E_s} = \frac{1}{8\pi^2 \text{SNR} B_{\text{eff}}^2} \quad (23)$$

where $B_{\text{eff}}^2 = \int_{-\infty}^{\infty} f^2 |S(f)|^2 df / \int_{-\infty}^{\infty} |S(f)|^2 df$ is the square of the effective bandwidth of $s(t)$, and the signal-to-noise ratio (SNR) is defined as

$$\text{SNR} = \frac{E_s}{N_0} = \frac{1}{N_0} \int_T s^2(t) dt = \frac{1}{N_0} \int_T p(t) dt \quad (24)$$

TABLE I
PARAMETERS USED IN THE SIMULATION

Parameter	Symbol	Value
Carrier frequency	f_0	77 GHz
BS antenna gain	G_{T}	5 dB
Bandwidth	W	4 GHz
Chirp time	T	1 ms
Target radius	r	0.05 m
Receiver's noise figure	F_{noise}	3 dB
Test angles	θ_{test}	$-(0:3:90)^\circ$
Parameter for F	q	0.57

where $p(t)$ is given by (22). Subsequently, the CRB of θ_0 can be obtained considering that $\text{CRLB}_{\theta_0} = \text{CRLB}_{t_0} \cdot (\partial\theta(t)/\partial t)^2$, being the derivative computed for $t = t_0$, where t_0 is the solution of (18) when $\theta(t_0)$ is set to θ_0 , which gives

$$t_0 = \frac{W}{2\beta} - [\sin(\theta_0) + \sin(\theta_{\text{inc}})] \frac{2\pi}{a_0 \lambda \beta}. \quad (25)$$

After some trigonometric manipulations and by defining $\text{K} = a_0 \lambda \beta / (2\pi)$, CRLB_{θ_0} becomes

$$\begin{aligned} \text{CRLB}_{\theta_0} &= \frac{\text{K}^2 / (8\pi^2 \text{SNR} B_{\text{eff}}^2)}{\cos^2(\theta_{\text{inc}}) - \text{K}^2 \left(\frac{W}{2\beta} - t_0\right)^2 + 2\text{K} \sin(\theta_{\text{inc}}) \left(\frac{W}{2\beta} - t_0\right)}. \end{aligned} \quad (26)$$

Finally, by replacing (25) in (26) we obtain

$$\text{CRLB}_{\theta_0} = \frac{\text{K}^2}{8\pi^2 \text{SNR} B_{\text{eff}}^2 \cos^2(\theta_0)}. \quad (27)$$

The last result indicates that the CRB on the estimation error variance of θ_0 worsens for large β and a_0 , i.e., for fast frequency sweeps of the chirp and higher frequency selectivity of the metaprism. Moreover, a larger effective bandwidth is obtained for narrow power profiles $p(t)$, i.e., smaller target footprints in the angular domain (small target and/or far target), and for small angle of view θ_0 .

V. NUMERICAL RESULTS

In this section, the evaluation of the angle estimation performance is reported. In the simulations, the target position was moved along an arc of 6 meters radius with angles ranging from 0 to -90° , with step 3° . The BS is at coordinates (3,0,3)m with respect to the reference system of Fig. 1. The metaprism was designed according to (19) with $\theta_m = 40^\circ$, thus spanning from -25° to -85° during a sweep of an FMCW chirp. The values of the parameters are shown in Tab. I.

In Fig. 4, examples of the received signal $y(t)$ and its envelope $z(t)$ are shown for some target test angles. It can be seen that $y(t)$ is negligible for angles that do not belong to the design range of the metaprism, i.e., $[-25^\circ : -85^\circ]$. Also, for each test angle, the maximum of the envelope corresponds to the time instant in which the instantaneous reflection angle of the metaprism $\theta(f(t))$, given by (17) and (18), is equal to test angle θ_0 . Subsequently, 1000 Monte Carlo iterations were considered to compute the root mean square error (RMSE) of the angle estimation of the proposed receiver for each target position. Fig. 5 shows the RMSE for different sizes

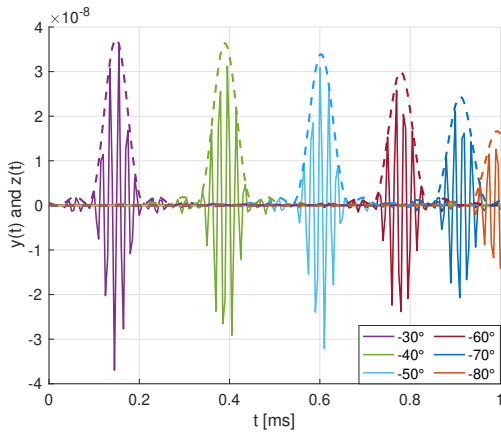


Fig. 4. Received signal $y(t)$ (continuous line) and its envelope $z(t)$ (dashed line), with $P_T = 15$ dBm and metaprim's size 20×50 cm².

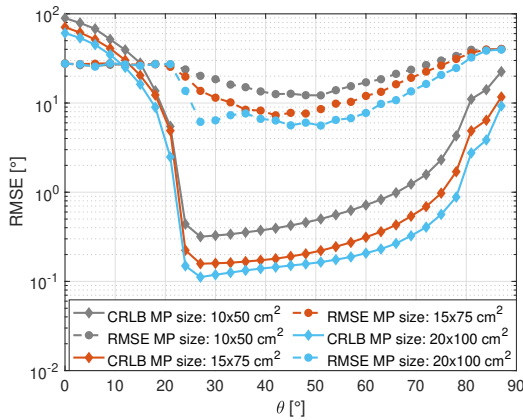


Fig. 5. CRLB and RMSE results varying the size of the metaprim (MP) with fixed $P_T = 15$ dBm.

of the metaprim, in particular, from 10×50 cm² (i.e., $N = 53$, $M = 257$) to 20×100 cm² (i.e., $N = 103$, $M = 515$). What emerges is that the best estimate of the angle, in the range where the metaprim has been designed, is less than 10° . Moreover, lower values of RMSE can be obtained by increasing the size of the metaprim. The square root of the CRB on angle estimation is also reported for comparison. The gap with respect to the performance of the proposed receiver has to be ascribed to the fact that the CRB intrinsically assumes that $s(t)$ is perfectly known at the receiver, which is not typically the case in realistic situations. Fig. 6 investigates the impact of the transmitted power on the performance with a metaprim's size of 20×50 cm². The results show that it is possible to achieve an estimation accuracy better than 1° with a typical power of $P_T = 20$ dBm. As regards the estimation of the range, simulation results indicate that, with the parameters considered, the RMSE of the range estimate is typically below 20 cm, thus confirming the capability of the proposed scheme to estimate both the angle and the range with high accuracy.

VI. CONCLUSIONS

In this work, an FMCW radar has been presented which exploits a passive frequency-selective non-reconfigurable meta-

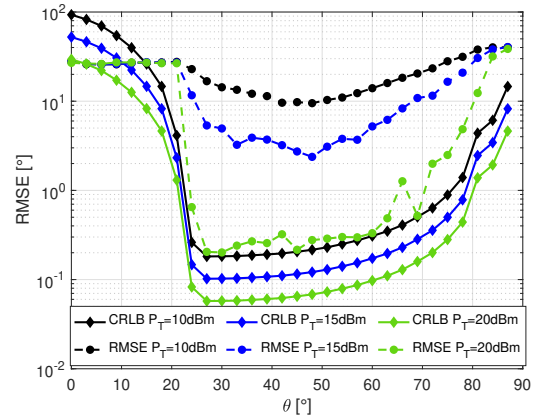


Fig. 6. CRLB and RMSE results varying P_T . Metaprim's size: 20×50 cm².

surface, called metaprim, to allow the localization of a target in NLOS localization. A modified FMCW receiver structure has been proposed which is capable of estimating simultaneously the angle and the range of the target using a conventional chirp signal. Results demonstrate that it is possible to obtain very accurate angle and range estimates without involving reconfigurable metasurfaces and multiple antennas at the BS.

ACKNOWLEDGMENT

This work was supported, in part, by the European Union under the Italian National Recovery and Resilience Plan (NRRP) of NextGenerationEU, partnership on "Telecommunications of the Future" (PE00000001 - program "RESTART"), and by the EU Horizon project TIMES (Grant no. 101096307).

REFERENCES

- [1] D. Dardari and N. Decarli, "Holographic communication using intelligent surfaces," *IEEE Commun. Mag.*, vol. 59, no. 6, pp. 35–41, 2021.
- [2] F. Liu, Y. Cui, C. Masouros, J. Xu, T. X. Han, Y. C. Eldar, and S. Buzzi, "Integrated sensing and communications: Towards dual-functional wireless networks for 6G and beyond," *IEEE J. Sel. Areas Commun.*, vol. 40, no. 6, pp. 1728–1767, 2022.
- [3] Y. Cui, F. Liu, X. Jing, and J. Mu, "Integrating sensing and communications for ubiquitous IoT: Applications, trends, and challenges," *IEEE Network*, vol. 35, no. 5, pp. 158–167, 2021.
- [4] E. Cisija, A. M. Ahmed, A. Sezgin, and H. Wymeersch, "RIS-aided mmWave MIMO radar system for adaptive multi-target localization," in *2021 Statistical Signal Processing Workshop (SSP)*. IEEE, July 2021, pp. 196–200.
- [5] D. Dardari, N. Decarli, A. Guerra, and F. Guidi, "LOS/NLOS near-field localization with a large reconfigurable intelligent surface," *IEEE Trans. on Wireless Commun.*, vol. 21, no. 6, pp. 4282–4294, 2022.
- [6] K. Keykhosravi, G. Seco-Granados, G. Alexandropoulos, and H. Wymeersch, "Ris-enabled self-localization: Leveraging controllable reflections with zero access points," in *IEEE International Conf. on Commun.*, vol. 2022, 2022, pp. 2852–2857.
- [7] D. Dardari and D. Massari, "Using metaprims for performance improvement in wireless communications," *IEEE Trans. on Wireless Commun.*, vol. 20, no. 5, pp. 3295–3307, 2021.
- [8] M. C. Budge and S. R. German, *Basic RADAR analysis*. Artech House, 2020.
- [9] H. Taub and D. L. Schilling, *Principles of communication systems*. McGraw-Hill Higher Education, 1986.
- [10] H. L. Van Trees, *Detection, estimation, and modulation theory, part I*. John Wiley & Sons, 2004.